IEEE Access
Multidisciplinary | Rapid Review | Open Access Journal

Received 24 August 2022, accepted 11 September 2022, date of publication 16 September 2022,
date of current version 28 September 2022.

Digital Object Identifier 10.1109/ACCESS.2022.3207284

RESEARCH ARTICLE

Stress Analysis of Tungsten Deposition in a 3D Trench Mold With Regard to Initial Nuclei Shape

JONG-SUNG LEE[1], SUNCHEUL KIM[2], DONGHOON HAN[2], MYOUNG-GYU LEE[1,3], AND YOUNG-CHANG JOO[1,3]

[1]Department of Materials Science & Engineering, Seoul National University, Gwanak-gu, Seoul 08826, South Korea
[2]Samsung Electronics Company Ltd., Hwaseong-si, Gyeonggi-do 18448, South Korea
[3]Research Institute of Advanced Materials, Seoul National University, Gwanak-gu, Seoul 08826, South Korea

Corresponding authors: Myoung-Gyu Lee (myounglee@snu.ac.kr) and Young-Chang Joo (ycjoo@snu.ac.kr)

This work was supported by the Samsung Electronics University Research and Development Program.

ABSTRACT Tungsten has been commonly used for fine interconnects due to its good gap-filling characteristics in 3D molds, such as trench patterns. However, tungsten shows high deposition stress. This causes mold distortion because tungsten has low ad-atom mobility, and diffusion-driven relaxation does not occur. To reduce tungsten's deposition stress, the shape of the nuclei can be controlled, which is an effective way to suppress the mechanical deformation caused by the formation of a grain boundary between free surfaces during the coalescence stage. In this study, elliptical tungsten nuclei with various aspect ratios, which suppress coalescence in the early stage of deposition, were proposed to reduce the deposition stress. Stress was calculated using the finite element method (FEM) in the range of 0.5 to 8 radius ratios of the tungsten nuclei. The bending of the trench mold was calculated due to tungsten stress and additional coalescence between films during the filling process. As a result, the wider the elliptical nucleus was, the lower the film stress, and mold bending between line patterns was also reduced. The defects in the depth and width of the periodic trench influenced the mold bending in the early growth stage and the stage of coalescence between films, respectively.

INDEX TERMS Finite element analysis, metallization, stress, thin films, tungsten.

I. INTRODUCTION

As the diminution of electronic devices progresses, the scale of their metal interconnects also decreases and becomes more precise. Thus, the fabrication technology used to form fine-pitch metal patterns has become very important [1], [2], [3]. Metal is deposited inside a trench-type pattern mold having a narrow width and a deep depth to form interconnections with a large cross-sectional area in a limited space. Tungsten shows good gap-filling characteristics due to its high step coverage obtained through chemical vapor deposition; thus, it has been used to fill the inside of a deep mold and make vertical structures with high aspect ratios, such as via and plug structures [4], [5], [6], [7]. Tungsten is commonly used as an interconnection metal for highly integrated patterns due to its advantage of being able to fill the inside of a deep trench mold with a narrow width and pitch.

However, when tungsten is used to fill a 3D trench mold with a high aspect ratio and narrow pitch, distortion, such as the bending of the mold, occurs by deposition stress in the metal thin films [8], [9], [10]. Fig. 1(a)-(c) is a schematic diagram showing the stage of stress evolution and the bending of the vertical trench mold when filling the trench and forming a line pattern with metal. The development of major tensile stress in trench mold bending is twofold. (1) The intergranular coalescence and corresponding stress are attributed to the deformation of the trench mold as the metal nuclei on the wall coalesce into a continuous thin film. (2) When the films on both walls are sufficiently grown and close to each other in the center of the trench, interfilm coalescence occurs through the formation of a grain boundary between the films, which reduces the free surface of the film. In the case of the deep trench structure for the line pattern, deposition stress causes

The associate editor coordinating the review of this manuscript and approving it for publication was Wen-Sheng Zhao.

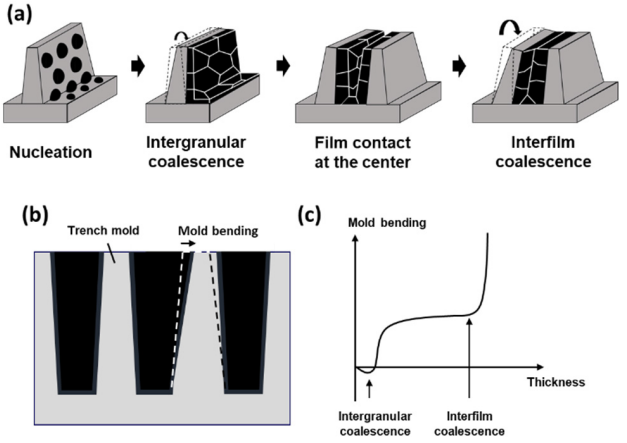

FIGURE 1. (a) Schematic of the stress evolution stage in the trench filling process that forms a line pattern with a high aspect ratio. Intergranular coalescence occurs only in the sidewall of the mold, and interfilm coalescence is caused by the attachment between the free surfaces on the tops of both films. (b) 2D Schematic illustration of mold bending due to film stress on the trench mold, which vertically separates the line pattern. (c) Schematic plot of mold bending caused by coalescence versus thickness.

the bending of the vertical mold, which separates the line patterns in Fig. 1(b). The vertical mold is bent, as shown in the plot schematic of Fig. 1(c), during the coalescence stage. Interfilm coalescence causes larger mold bending than intergranular coalescence because the area of the grain boundary formed between films is much wider than that of intergranular coalescence. Deposition stress and mold bending lead to mechanical failure, such as the leaning and poor gap filling caused by the bending of the vertical trench mold [9], [11].

The main source of tensile stress during metal film deposition is the mechanical deformation of metal nuclei due to coalescence, which is called the zipping phenomenon [12], [13], [14], [15], [16]. The nuclei deform to reduce the high-energy free surface, while they also form grain boundaries with relatively low energy when the nuclei contact each other. Tensile stress from coalescence has been estimated by both analytical solutions [17] or numerical methods, such as the finite element method (FEM) [13], [14] and molecular dynamics (MD) analysis [18]. These models calculated the deposition stress of high ad-atom mobility metals such as aluminum, silver, and copper, which show low stress due to diffusion-driven relaxation under low temperature deposition [19], [20], [21], [22].

However, previous zipping models of high ad-atom mobility metals are not suitable for calculating the stress of refractory metals such as tungsten, molybdenum and ruthenium. Tungsten shows higher deposition stress because of its low ad-atom mobility and high surface energy. Mechanical deformation due to zipping is continuous even after the film is formed, and diffusion-driven relaxation does not occur under the low-temperature deposition of tungsten [21], [23]. Therefore, stress control in the early stage, such as the metal nucleation stage, is more important to reduce the deposition stress than in the case of high ad-atom mobility metals.

Our study proposes a method for calculating deposition stress considering the continuous stress evolution (intergranular coalescence) and additional stress evolution of a 3D structure (interfilm coalescence). The initial shape of the tungsten nuclei was controlled to suppress zipping deformation and reduce the stress of the tungsten film in the intergranular coalescence stage. The zipping phenomenon was simulated and analyzed using finite element (FE) simulation, and the stress depending on the nuclei shape was calculated during the growth of the tungsten film. Based on the film stress, the mold bending of the vertical mold was calculated by a 2D cross-sectional model of a deep trench. In addition, the mold bending resulting from interfilm coalescence between the films on the walls in the middle of the trench was analyzed.

II. SIMULATION DETAILS

Finite element (FE) simulation was conducted using a static implicit solver, ABAQUS/Standard (Dassault System, France), which has advantages for structural analysis with solid-solid contacts under nonlinear deformation. All simulations were performed in 2D models with plane strain elements (CPE4 in ABAQUS), which is a 2D-type element that is used in cross-sections in thick structures and is assumed to have zero strain in the thickness direction [24]. The material properties of tungsten were assumed to exhibit linear isotropic elasticity with a Young's modulus of 300 GPa and Poisson's ratio of 0.28 [25]. The height of the tungsten nucleus is $t_i = 30$ Å, and the radius of the width, r, is 15∼240 Å, as shown in Fig. 2(a). The mechanical properties of the Si trench mold were also considered to exhibit linear isotropic elasticity with a Young's modulus and Poisson's ratio of 127 GPa and 0.278, respectively [26]. Two cases of mold pattern defects with depth and width differences from the ideal pattern are presented to calculate mold bending from the asymmetric bending moment in Fig. 2(b). There are two major stress generation stage analysis models: intergranular coalescence and interfilm coalescence, and the nuclei and film on mold models shown in Fig. 2(a) and (b) were used, respectively. The stress calculation proceeded in the order of the flow chart of Fig. 3(c). Stress calculation was conducted by an elastic model under static conditions, the boundary condition between the nucleus and the mold at the bottom of the mold was pinned, and an x-axis symmetric boundary condition was given to both sides of the model for periodic planes. Then, the zipping analysis was performed by applying the boundary condition of the force that the metal surfaces feature traction toward each other. The strain energy and zipping distance (z_0) were calculated by applying a surface traction from 0 to 20 GPa on the surface of the nucleus, depending on the width-to-height ratios of the nuclei island (r/t_i). The energy change from zipping was calculated by equation (1), which considers decreasing free surface energy and increasing grain boundary energy due to the zipping

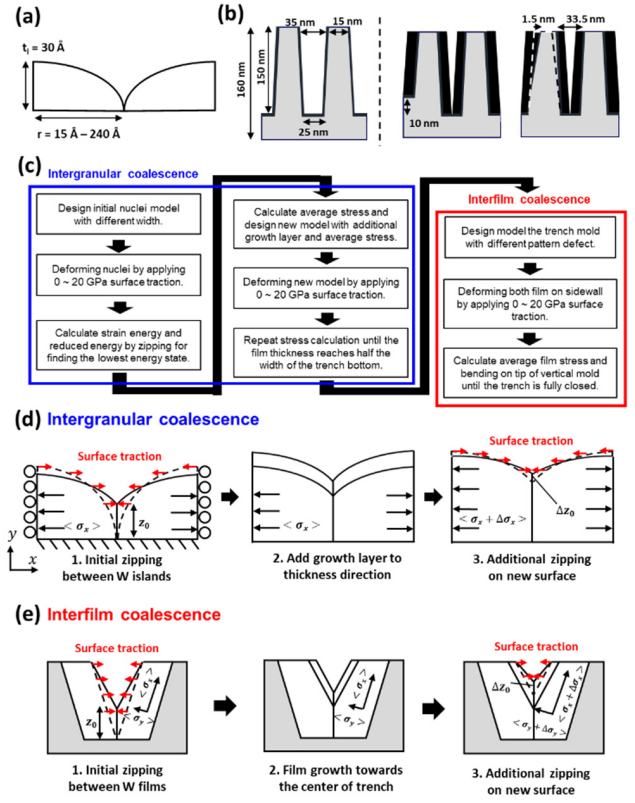

FIGURE 2. **(a) Schematic of the model used to calculate film stress in intergranular coalescence caused by contact between metal nuclei, depending on the ratio of width-to-height (r/t_i) of nuclei. Surface traction on the nuclei surface was applied to calculate the average stress and strain energy due to intergranular coalescence. (b) Schematic of the trench mold used to calculate mold bending due to interfilm coalescence during the trench filling process. Mold bending was calculated under two cases of pattern defect: depth difference and width difference. (c) The flow chart of the simulation procedure of intergranular coalescence (blue box) and interfilm coalescence (red box), respectively. (d) Schematic image of the simulation model of intergranular coalescence between tungsten islands during film growth and (e) the simulation model for interfilm coalescence occurring in the center of the trench mold to form a line pattern. Both models were deformed by surface traction to calculate film stress and mold bending.**

process [17]:

$$\Delta E_{zipping} = z_0 \left(\gamma_{gb} - 2\gamma_s\right) \tag{1}$$

where γ_{gb} is the grain boundary energy and γ_s is the surface energy of tungsten, calculated as 1.08 J/m^2 and 2.83 J/m^2, respectively [27]. By balancing the strain energy and reduced energy by zipping, the average stress could be calculated from the state with the lowest energy.

For zipping and stress analysis during film growth, a stress-free growth layer with a thickness of 2.24 Å was added by calculating the interplanar distance of the tungsten (110) plane, and surface traction was applied to the new surface. Then, the average stress in the film was calculated through the same zipping analysis. By calculating the average stress through incremental growth, which was repeated until the target thickness just before contact at the center of the trench, the stress evolution during film growth was obtained. The schematic procedure for the calculation of stress during film growth is shown in Fig. 2(c). The initial value of the film stress is negative (compressive stress) due to the surface tension [28], [29], which can be calculated with equation (2) [21]:

$$\Delta P = -f\frac{dA}{dV} \tag{2}$$

where P is the internal pressure, f is the surface tension, A is the surface area of the nucleus, and V is the volume of the nucleus.

The zipping between the tops of the films was also analyzed, and the average stress in the horizontal and vertical directions inside the film was calculated, as shown Fig. 2(d). Surface traction was applied to the surface of the film, and strain energies due to deformation and z_0, which formed as a grain boundary, were calculated. The average stress was also calculated at the state when the balance between the strain energy and the energy reduced by grain boundary formation was lowest. To quantify the bending of the trench mold due to geometrical defects, mold bending was defined in this study by measuring the displacement of the tip of the vertical mold between the trenches during the growth of the tungsten film on each wall until the pattern was closed.

Intergranular zipping simulations for molybdenum and ruthenium, which have the same growth mechanism as tungsten, were performed. The stress depending on the nuclei shape was calculated by applying the mechanical properties of molybdenum and ruthenium. The Young's moduli of molybdenum and ruthenium were 324 GPa and 414 GPa, respectively, and Poisson's ratios were 0.29 and 0.25, respectively [30]. The surface energies of molybdenum and ruthenium were 2.05 J/m^2 and 3.08 J/m^2, and the grain boundary energy was 0.61 J/m^2 and 1.12 J/m^2, respectively [27], [31], [32].

III. RESULTS AND DISCUSSION

Fig. 3(a) and (b) illustrate the FEM simulation results of the (normalized) zipping distance and the (normalized) average nuclei stress, which show the nuclei shape effect on intergranular coalescence at initial contact. The zipping distance and average stress decrease as the ratio r/t_i increases, which corresponds to the increased principal axis of the elliptical shape of the nuclei along the horizontal direction. A wide elliptical nucleus can be formed in the horizontal direction instead of a spherical one by controlling the nucleation of the metal nucleus [33], [34]. This leads to reduced stress in the nuclei and substrate distortion by the suppressed zipping. When the r/t_i ratio increases above 5, zipping becomes negligible, and stress is not generated. This is because the strain energy due to deformation increases significantly, while the reduced energy due to grain boundary formation decreases as the nucleus becomes wider elliptically. Note that the first and second contributions correspond to a counter force of the zipping phenomenon and a driving force of the zipping phenomenon, respectively. Therefore, zipping is suppressed

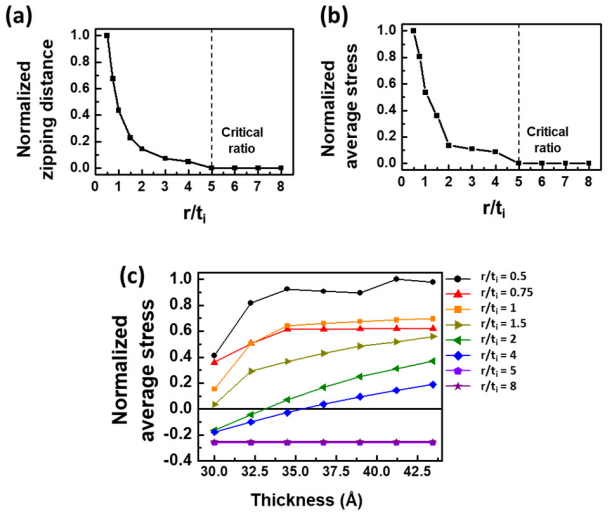

FIGURE 3. FEM simulation results of the intergranular coalescence stage. (a) Normalized zipping distance (z_0) and (b) normalized average stress when zipping occurs at the initial contact between nuclei depending on the r/t_i of the nuclei. (c) Normalized average stress depending on r/t_i during film growth after contact between nuclei.

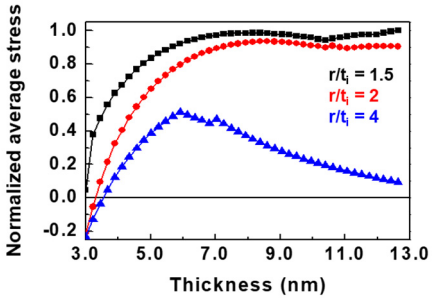

FIGURE 4. Finite element simulation result of stress evolution during growth after forming a continuous film. The graphs in the figure represent the stresses for different r/t_i values, where the initial nuclei have r/t_i values of 1.5 (black), 2 (red), and 4 (blue).

as the nuclei converge to an ellipse with a wider shape, and the shape factor with a r/t_i above 5 can be regarded as the critical ratio.

Fig. 3(c) is a simulation result of the normalized average stress in the early growth stage depending on the r/t_i ratio. Low compressive stress is generated by the surface tension of tungsten at first, and then tensile stress begins to increase rapidly through zipping after nuclei contact. Even during thickening, a large stress is continuously generated because a low r/t_i shape is advantageous for grain boundary formation through zipping deformation. However, in the case of a higher r/t_i than the critical ratio, the initial compressive stress is not compensated for and affects the distortion of the substrate or mold. It is necessary to optimize the initial deposition conditions to balance the compressive stress due to the surface tension and the tensile stress due to zipping.

Fig. 4 shows the simulated normalized average stress during growth as the film thickness increases. The graphs in the figure represent the stress evolution after forming continuous films with different r/t_i values of 1.5, 2, and 4. As the thickness of the tungsten film increased, the zipping continued to generate tensile stress in the film, and the stress decreased as the r/t_i value increased. Among the three curves in Fig. 4, the tensile stress in the case of $r/t_i = 4$ decreased at a thickness of 6 nm, where zipping during thickening stopped when the thin film formed a flattened shape. This simulation result indicates that the stress can be relaxed by suppressing the zipping or by controlling the shape of the elliptical nucleus with a high r/t_i ratio.

Fig. 5(a) and (b) show the mold bending (normalized by maximum bending after pattern closure) caused by the differences in depth (case 1) and width (case 2) from the ideal mold geometry, respectively. The two figures show that the distortion of the vertical mold represents either a gradual (Fig. 5(a)) or constant (Fig. 5(b)) increase before the tungsten film begins zipping at the center of the trench mold (or film thickness of approximately 12.5 nm). In both cases 1 and 2, the mold bending resulting from the interfilm coalescence is larger than that resulting from the intergranular coalescence. This can be explained by the fact that a larger free surface can be reduced by mold bending through interfilm coalescence. In the stage of intergranular coalescence, a different trend of mold bending was observed for the two defect patterns. When the mold has a depth difference (case 1), the mold is continuously bent as the film stress increases, while the bending of the mold with a width difference is nearly independent of the film growth. The main factor in mold bending by intergranular coalescence is the difference in the bending moment produced by the thin film stress on both walls of the mold. When there is a difference in depth in the trench mold, the areas of tungsten film covering the mold walls are different, which results in the difference in depth. Therefore, this unbalanced film growth (equivalently asymmetric stress distribution on each wall) causes additional bending. On the other hand, when two thin films contact the center of the trench by zipping, abrupt changes in the model bending occur for the case of mold width difference (Fig. 5(b)). When the mold is already bent, it is easier to form an additional interface, which appears to induce more mold bending. Fig. 5(c) shows the mold bending assuming both defects (depth and width) exist. In this case, the mold bending by the depth difference becomes more dominant during film growth on the wall, but the bending by the width difference increases after the films contact the center of the mold.

In addition, the cross-sectional area of the metal interconnects was calculated to determine the electrical resistance. The pattern defect with a depth difference of 10 nm and a width difference of 1.5 nm decreases the cross-sectional area of the metal line compared to a symmetric trench without a pattern defect. If there is no stress on the film and no bending

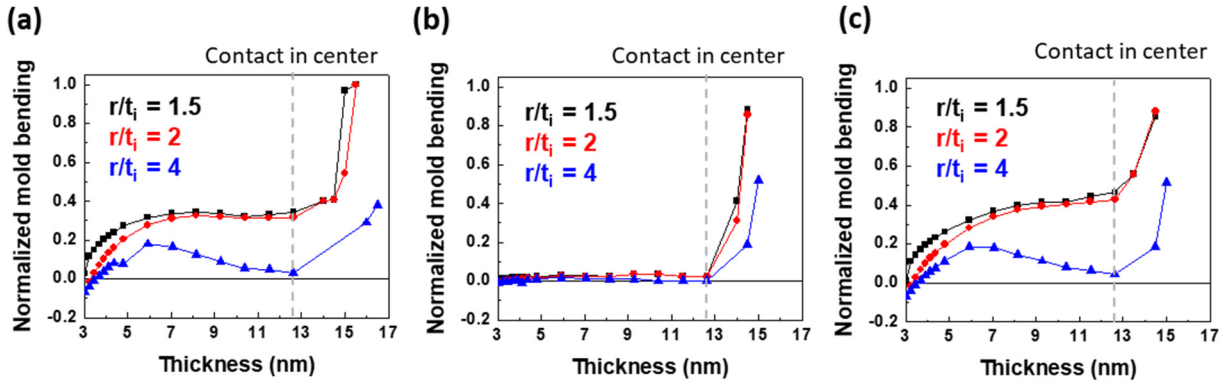

FIGURE 5. Simulation results for mold bending by the pattern defects of two cases, i.e., the results of the mold bending of an Si mold due to film stress and interfilm coalescence. An asymmetric structure was used to calculate mold bending due to patterning error or other defects: (a) depth difference, (b) width difference and (c) both differences.

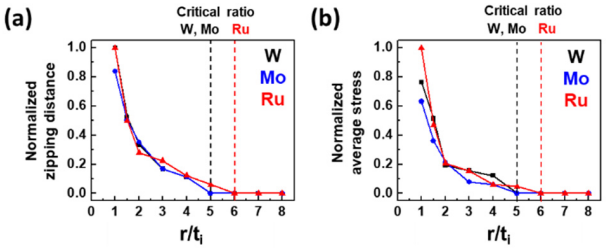

FIGURE 6. FEM simulation results of initial zipping depending on the r/t_i of the tungsten (black), molybdenum (blue), and ruthenium (red) nuclei: (a) normalized zipping distance and (b) normalized average stress.

of the mold, the cross-sectional area is reduced by 2.53% compared to a trench without a pattern defect. However, in the case of $r/t_i = 4$, where the stress is lowest, the cross-sectional area decreases by 5.26%, and in the case of $r/t_i = 1.5$, where the stress occurs the most, the cross-sectional area decreases by 6.83%. In addition, when considering the early closing of the upper part due to overhang, the film stress affects a greater conductivity decrease due to a lower cross-sectional area.

Fig. 6 illustrates the simulation results of initial zipping on molybdenum and ruthenium, which have the same mechanism of stress evolution as tungsten. Fig. 6(a) and (b) shows the (normalized) zipping distance and the (normalized) average nuclei stress of tungsten, molybdenum, and ruthenium using our simulation method. Molybdenum has a similar Young's modulus to tungsten and lower γ_s and γ_{gb} than tungsten. Ruthenium has a higher Young's modulus, γ_s, and γ_{gb} than tungsten. Both molybdenum and ruthenium showed the same shape dependence as tungsten, and the zipping stress decreased as the nucleus became wider. However, molybdenum showed a lower zipping distance and stress because the driving force of zipping decreased in the molybdenum case. When the grain boundary formed due to zipping, the energy reduction of molybdenum was smaller than that of tungsten because of its low surface energy. On the other hand, the driving force of zipping is stronger in the ruthenium case, and the zipping distance and stress increased. Furthermore, higher stress is also generated because of the higher Young's modulus of ruthenium, and the critical ratio of r/t_i where zipping does not occur increased from 5 to 6, confirming that wider nuclei are needed to minimize stress in ruthenium.

Our stress calculation model has a limitation attributed to the assumptions made in the finite element analysis. First, in the finite element simulation, the materials are all considered continuum bodies, and the interactions of the surface atoms during the zipping process are simplified as tied boundary conditions. Additionally, the anisotropy of the tungsten film is not considered, although crystalline solids such as tungsten have strong anisotropy at the grain scale. Therefore, more accurate analysis can be achieved if these simplifying assumptions are removed by introducing atomic level computations, such as density functional theory or molecular dynamics, for the calculation of zipping stress by interatomic interactions. Furthermore, for the stress calculation in the case of a hole-type structure such as deep via and plug, all three-dimensional zipping between the thin films growing on all sidewalls should be calculated, and a 3D model is needed.

IV. CONCLUSION

Tungsten exhibits higher stress than conventional interconnection metals when it is used as a gap filler by chemical vapor deposition. High deposition stress by zipping results in severe distortion of the thin vertical mold, which is designed to fabricate interconnects with fine pitch. Our study based on the shape optimization of tungsten nuclei through finite element simulation proposes elliptical nucleation with high width, which is intended to relax the zipping stress during growth on the trench mold. In the simulation, two sources of vertical mold distortion were investigated: the film stress induced by zipping between the two neighboring nuclei and the secondary zipping stress resulting from the coalescence

between the films in the trench. The results show that the tungsten film with low zipping stress induced by introducing an elliptical nuclei shape can be effectively suppress the distortion of the mold. For next-generation interconnect metals, such as Ru and Mo, which have similar zipping mechanisms to tungsten, high deposition stress will cause pattern distortion issues. Tungsten is widely used in the filling process, and many studies have been conducted to measure the deposition stress. However, there are fewer studies on stress analysis on next-generation interconnect metals. Therefore, the stress analysis model proposed in this study can be extended to provide guidelines to predict and reduce deposition stress in fine patterns by metallization.

REFERENCES

[1] S. E. Thompson and S. Parthasarathy, "Moore's law: The future of Si microelectronics," *Mater. Today*, vol. 9, no. 6, pp. 20–25, Jun. 2006, doi: 10.1016/S1369-7021(06)71539-5.

[2] J. U. Knickerbocker, P. S. Andry, B. Dang, R. R. Horton, C. S. Patel, R. J. Polastre, K. Sakuma, E. S. Sprogis, C. K. Tsang, B. C. Webb, and S. L. Wright, "3D silicon integration," in *Proc. 58th Electron. Compon. Technol. Conf.*, Lake Buena Vista, FL, USA, 2008, pp. 538–543.

[3] M. Koyanagi, T. Fukushima, and T. Tanaka, "High-density through silicon vias for 3-D LSIs," *Proc. IEEE*, vol. 97, no. 1, pp. 49–59, Jan. 2009, doi: 10.1109/JPROC.2008.2007463.

[4] G. Ruhl, B. Fröschle, P. Ramm, A. Intemann, and W. Pamler, "Deposition of titanium nitride/tungsten layers for application in vertically integrated circuits technology," *Appl. Surf. Sci.*, vol. 91, no. 1, pp. 382–387, Oct. 1995, doi: 10.1016/0169-4332(95)00151-4.

[5] S. B. Herner, "Homogeneous tungsten chemical vapor deposition on silane pretreated titanium nitride," *Electrochem. Solid-State Lett.*, vol. 2, no. 8, p. 398, May 1999, doi: 10.1149/1.1390850.

[6] M. Koyanagi, T. Nakamura, Y. Yamada, H. Kikuchi, T. Fukushima, T. Tanaka, and H. Kurino, "Three-dimensional integration technology based on wafer bonding with vertical buried interconnections," *IEEE Trans. Electron Devices*, vol. 53, no. 11, pp. 2799–2808, Oct. 2006, doi: 10.1109/TED.2006.884079.

[7] F. Liu, R. R. Yu, A. M. Young, J. P. Doyle, X. Wang, L. Shi, K. N. Chen, X. Li, D. A. Dipaola, D. Brown, and C. T. Ryan, "A 300-mm wafer-level three-dimensional integration scheme using tungsten through-silicon via and hybrid Cu-adhesive bonding," in *Proc. IEEE Int. Electron Devices Meeting*, San Francisco, CA, USA, Dec. 2008, pp. 1–4.

[8] D. H. Triyoso, T. B. Dao, T. Kropewnicki, F. Martinez, R. Noble, and M. Hamilton, "Progress and challenges of tungsten-filled through-silicon via," in *Proc. IEEE Int. Conf. Integr. Circuit Design Technol.*, Grenoble, France, Jun. 2010, pp. 118–121.

[9] M.-G. Sung, Y. S. Kim, and S.-K. Park, "Stress induced self aligned contact failure during tungsten-poly gate process in sub-60 nm memory device," in *Proc. 18th IEEE Int. Symp. Phys. Failure Anal. Integr. Circuits (IPFA)*, Incheon, South Korea, Jul. 2011, pp. 1–4.

[10] T. Dao, D. H. Triyoso, R. Mora, T. Kropewnicki, B. Griesbach, D. Booker, M. Petras, and V. Adams, "Thermo-mechanical stress characterization of tungsten-fill through-silicon-via," in *Proc. Int. Symp. VLSI Technol. Syst. Appl.*, Taiwan, Apr. 2010, pp. 96–99.

[11] K. Kim, "Technology for sub-50 nm DRAM and NAND flash manufacturing," in *IEDM Tech. Dig.*, Washington, DC, USA, 2005, pp. 323–326.

[12] W. D. Nix, "Mechanical properties of thin films," *Metall. Trans. A*, vol. 20, no. 11, p. 2217, Nov. 1989, doi: 10.1007/BF02666659.

[13] S. C. Seel, C. V. Thompson, S. J. Hearne, and J. A. Floro, "Tensile stress evolution during deposition of Volmer–Weber thin films," *J. Appl. Phys.*, vol. 88, no. 12, pp. 7079–7088, Dec. 2000, doi: 10.1063/1.1325379.

[14] S. C. Seel and C. V. Thompson, "Tensile stress generation during island coalescence for variable island-substrate contact angle," *J. Appl. Phys.*, vol. 93, no. 11, pp. 9038–9042, Jun. 2003, doi: 10.1063/1.1571964.

[15] L. B. Freund and E. Chason, "Model for stress generated upon contact of neighboring islands on the surface of a substrate," *J. Appl. Phys.*, vol. 89, no. 9, pp. 4866–4873, May 2001, doi: 10.1063/1.1359437.

[16] M. H. Grabow and G. H. Gilmer, "Thin film growth modes, wetting and cluster nucleation," *Surf. Sci.*, vol. 194, no. 3, pp. 333–346, Jan. 1988, doi: 10.1016/0039-6028(88)90858-8.

[17] W. D. Nix and B. M. Clemens, "Crystallite coalescence: A mechanism for intrinsic tensile stresses in thin films," *J. Mater. Res.*, vol. 14, no. 8, pp. 3467–3473, Aug. 1999, doi: 10.1557/JMR.1999.0468.

[18] H. Zheng, "Molecular dynamic simulation of thin film growth stress evolution," M.S. thesis, Dept. Mech. Eng. Mech., Lehigh Univ., Ann Arbor, MI, USA, 2011.

[19] R. Abermann and R. Koch, "The internal stress in thin silver, copper and gold films," *Thin Solid Films*, vol. 129, pp. 71–78, Jul. 1985, doi: 10.1016/0040-6090(85)90096-3.

[20] A. L. Shull and F. Spaepen, "Measurements of stress during vapor deposition of copper and silver thin films and multilayers," *J. Appl. Phys.*, vol. 80, no. 11, pp. 6243–6256, Dec. 1996, doi: 10.1063/1.363701.

[21] R. C. Cammarata, T. M. Trimble, and D. J. Srolovitz, "Surface stress model for intrinsic stresses in thin films," *J. Mater. Res.*, vol. 15, no. 11, pp. 2468–2474, Nov. 2011, doi: 10.1557/JMR.2000.0354.

[22] A. Saedi and M. J. Rost, "Thermodynamics of deposition flux-dependent intrinsic film stress," *Nature Commun.*, vol. 7, no. 1, p. 10733, Feb. 2016, doi: 10.1038/ncomms10733.

[23] G. J. Leusink, T. G. M. Oosterlaken, G. C. A. M. Janssen, and S. Radelaar, "The evolution of growth stresses in chemical vapor deposited tungsten films studied byinsituwafer curvature measurements," *J. Appl. Phys.*, vol. 74, no. 6, pp. 3899–3910, Sep. 1993, doi: 10.1063/1.354485.

[24] J. N. Reddy, *Introduction to the Finite Element Method*. New York, NY, USA: McGraw-Hill, 2019.

[25] M. Bauccio, *ASM Metals Reference Book*. Almere, NL, USA: ASM International, 1993.

[26] L. Gan, B. Ben-Nissan, and A. Ben-David, "Modelling and finite element analysis of ultra-microhardness indentation of thin films," *Thin Solid Films*, vols. 290–291, pp. 362–366, Dec. 1996, doi: 10.1016/S0040-6090(96)08972-9.

[27] E. N. Hodkin, M. G. Nicholas, and D. M. Poole, "The surface energies of solid molybdenum, niobium, tantalum and tungsten," *J. Less Common Met.*, vol. 20, no. 2, pp. 93–103, Feb. 1970, doi: 10.1016/0022-5088(70)90093-7.

[28] R. Abermann, R. Kramer, and J. Mäser, "Structure and internal stress in ultra-thin silver films deposited on MgF_2 and SiO substrates," *Thin Solid Films*, vol. 52, no. 2, pp. 215–229, Jul. 1978, doi: 10.1016/0040-6090(78)90140-2.

[29] R. C. Cammarata, "Surface and interface stress effects in thin films," *Prog. Surf. Sci.*, vol. 46, no. 1, pp. 1–38, May 1994, doi: 10.1016/0079-6816(94)90005-1.

[30] R. B. Ross, *Metallic Materials Specification Handbook*. London, U.K.: Chapman Hall, 1992.

[31] F. Aqra and A. Ayyad, "Surface energies of metals in both liquid and solid states," *Appl. Surf. Sci.*, vol. 257, no. 15, pp. 6372–6379, May 2011, doi: 10.1016/j.apsusc.2011.01.123.

[32] H. Zheng, X.-G. Li, R. Tran, C. Chen, M. Horton, D. Winston, K. A. Persson, and S. P. Ong, "Grain boundary properties of elemental metals," *Acta Mater.*, vol. 186, pp. 40–49, Mar. 2020, doi: 10.1016/j.actamat.2019.12.030.

[33] M. S. Marangon, G. Queirolo, and C. Savoia, "Nucleation and growth of CVD-W on TiN studied by X-ray fluorescence spectrometry," *Appl. Surf. Sci.*, vol. 91, no. 1, pp. 157–161, Oct. 1995, doi: 10.1016/0169-4332(95)00112-3.

[34] C. M. McConica and K. Cooper, "Tungsten nucleation on thermal oxide during LPCVD of tungsten by the hydrogen reduction of tungsten hexafluoride," *J. Electrochem. Soc.*, vol. 135, no. 4, pp. 1003–1008, Apr. 1988, doi: 10.1149/1.2095756.

JONG-SUNG LEE received the B.S. degree in material science and engineering from Seoul National University, Seoul, South Korea, in 2017, where he is currently pursuing the Ph.D. degree in material science and engineering with the Department of Materials Science and Engineering. His research interests include stress analysis using finite element analysis and the reliability of electronic material and packages.

SUNCHEUL KIM received the B.S. and Ph.D. degrees in material science engineering from the Korea Advanced Institute of Science and Technology, Daegeon, South Korea, in 2011 and 2017, respectively. From 2017 to 2022, he was a Staff Engineer at Samsung Electronics, Gyeoggi-do, South Korea, where he has been a Principal Engineer, since 2022. His research interests include metal deposition and development of electronic devices, such as DRAM and VNAND devices.

DONGHOON HAN received the B.S. and Ph.D. degrees in material science and engineering from Seoul National University, Seoul, South Korea, in 2005 and 2011, respectively. From 2011 to 2017, he was a Staff Engineer at Samsung Electronics, Gyeoggi-do, South Korea, where he has been a Principal Engineer, since 2018. His research interests include metal deposition and development of deposition equipments for electronic devices, such as DRAM and VNAND.

MYOUNG-GYU LEE received the B.S. and M.S. degrees in fiber and polymer engineering and the Ph.D. degree in material science and engineering from Seoul National University, Seoul, South Korea, in 1997, 1999, and 2004, respectively.

In 2007, he completed his postdoctoral research with The Ohio State University, Columbus, OH, USA. From 2007 to 2010, he was with the Korea Institute of Materials Science, Gyeongsangnam-do, South Korea. From 2010 to 2014, he was an Associate Professor with POSTECH, Gyeongbuk, South Korea. From 2014 to 2018, he was with Korea University, Seoul, as an Associate Professor. Since 2018, he has been with the Department of Materials Science and Engineering, Seoul National University, as a Professor. His research interests include computational mechanics and modeling for metals and fracture mechanics for ductile alloys and their applications.

YOUNG-CHANG JOO received the B.S. and M.S. degrees in metallurgical engineering from Seoul National University, Seoul, South Korea, in 1987 and 1989, respectively, and the Ph.D. degree from the Massachusetts Institute of Technology, Cambridge, MA, USA, in 1995.

In 1997, he completed his postdoctoral research with the Max-Planck-Institut für Metallforschung, Stuttgart, Germany. In 1999, he was with Advanced Micro Devices Inc., Sunnyvale, CA, USA. Since 1999, he has been with the Department of Materials Science and Engineering, Seoul National University, as a Professor. His research interests include the reliability and development of next-generation electronic materials and devices.